LANDSLIDE SUSCEPTIBILITY ANALYSIS OF JUGAL RURAL MUNICIPALITY, SINDHUPALCHOK

Prateek Pradhan[1], **Bhim Kumar Dahal**[1] *

[1] Department of Civil Engineering, Pulchowk Campus, IOE, Tribhuvan University

Abstract

Hilly and mountainous areas of Nepal, with challenging terrain, young geology, and heavy monsoon rainfall, are susceptible to landslides and slope instability. To analyze and prepare landslide susceptibility maps, this study selects a typical hilly area, the Jugal Rural Municipality in Sindhupalchok district. Twelve factors contributing to landslides were considered, including slope, aspect, elevation, geology, land use, proximity to roads and drainage, plan curvature, profile curvature, NDVI (Normalized Difference Vegetation Index), soil type and rainfall. Moreover, 286 landslides were identified using high-resolution satellite imagery and field verification as the landslide inventory. These landslides were then randomly divided into two sets: 70% for training and 30% for validation. Bivariate statistical analysis was performed using factor maps and the landslide inventory map. Notably, the analysis revealed a Prediction Rate (PR) of 9.35 for 'Land use', the highest among all factors considered. Since land use is a dynamic factor, we recommend conducting an analysis of land use changes and their impact on landslide susceptibility. Such an assessment would be invaluable during the planning and execution phases of development projects in Nepal's disaster-prone regions.

Keywords: Landslides, Susceptibility, Jugal, Sindhupalchok

1. Introduction

Nepal has a high climate risk and is ranked 9th as per the Global Climate Risk Index 2020, which evaluates the impact of meteorological events on economic losses and human fatalities (Sönke et al., 2015). The occurrence of natural hazards like landslides is governed by triggers and causative factors. Landslides in Nepal mainly result from a combination of natural factors like steep slopes, fragile geology, heavy and irregular rainfall, and human factors such as deforestation, unplanned settlements, improper land use, and haphazard infrastructure development (Uprety et al., 2020). In 2020, landslides caused 303 deaths, 64 people went missing, and 226 were injured nationwide (MoHA, 2020).

Nepal experiences approximately 12,000 landslides, both small and large-scale annually (Bhusal, 2016). Over the past decade, data reveals an increasing trend in landslide-related deaths and affected families, particularly after the 2015 earthquake and Sindhupalchok district had the highest fatality count, with 3,575 deaths, following the earthquake (MoHA, 2022). The district, as well as areas with haphazard infrastructure development like road construction without proper environmental considerations, have witnessed a noticeable surge in landslides, indicating a clear correlation (McAdoo et al., 2018; Paudyal et al., 2023). The Lidi landslide in Jugal in 2020 can be attributed in part to the two days of heavy rainfall that saturated the slopes, reducing the soil's safety margin.

In addition to earthquake impacts, erratic rainfall, poorly planned infrastructure, and improper farming practices make the region more prone to landslides.

Many researchers are using susceptibility analysis as a helpful tool for managing landslide hazards. These maps indicate the likelihood of landslides happening in a specific area. They are prepared by predicting landslides spatial distribution, assuming that future landslides will occur under similar conditions as in the past (Martha et al., 2013). In a study, the Frequency Ratio (FR) model was implemented for landslide susceptibility mapping and was compared with

*Corresponding author: Bhim Kumar Dahal
Department of Civil Engineering, Pulchowk Campus, IOE, TU
Email: bhimd@pcampus.edu.np
(Received: Sept. 27, 2023, Accepted: Dec. 06, 2023)
https://doi.org/10.3126/jsce.v10i1.61019

the Logistic Regression model (Regmi et al., 2014). Different landslide susceptibility analysis methods were evaluated in Bagmati Rural Municipality where the FR method also showed good results employing remote sensing (RS) and geographic information system (GIS) techniques to identify potential landslide-prone areas in Nepal (Thapa et al., 2022).

1.1. Study area

The Jugal Rural Municipality covers a total area of 592 km2 and is divided into 7 wards. Sindhupalchowk was among the worst-hit districts over the years, with a total of 289 fatalities and 685 affected families (MoHA, 2022). The landslides continue to impact infrastructure such as hill roads and settlements. The increased frequency of landslides can be attributed to growth of unplanned settlement and unregulated infrastructure development. Location of the study area is presented in Figure 1.

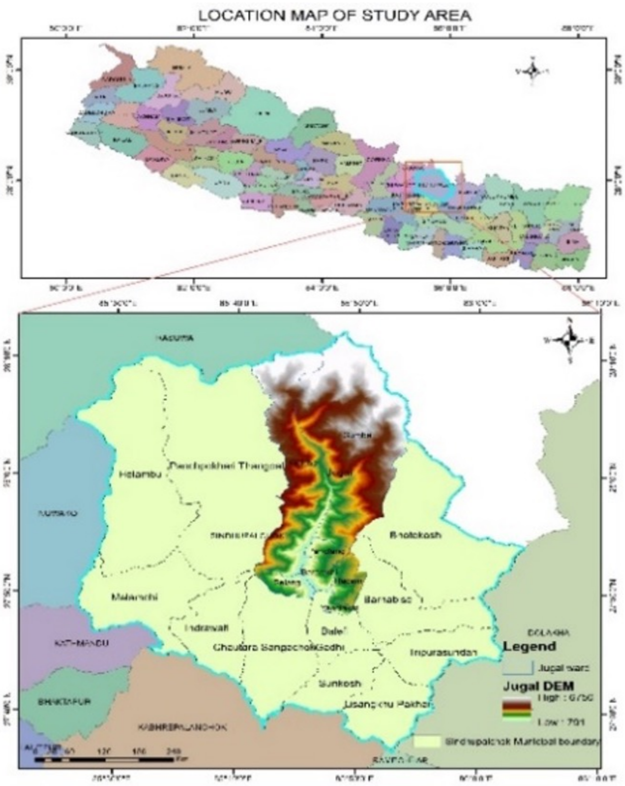

Figure 1. Location map of study area

2. Data and Methodology

The methodology of study is summarized in Figure 2.

GIS and Remote Sensing (RS) are highly effective tools for evaluating risk and managing natural hazards, especially when dealing with parameters with high spatial variability. Various literature have suggested that the data set ratio of

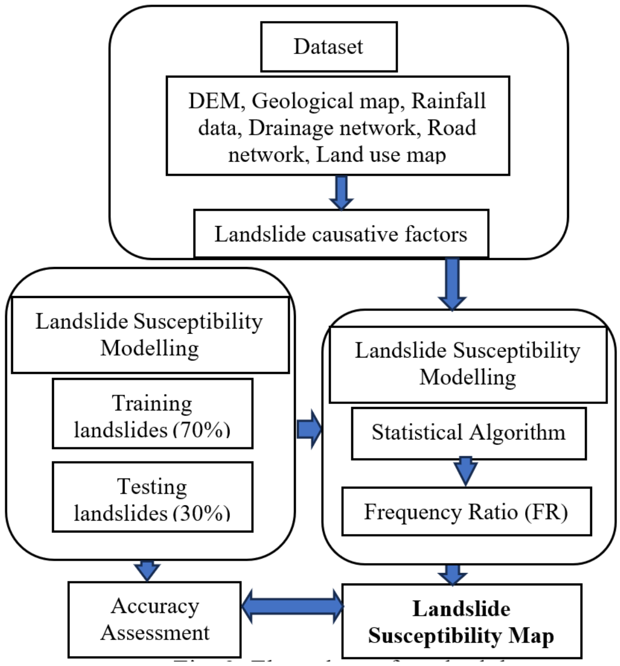

Figure 2. Methodology of the present study

70:30 because the 70% data set is considered sufficient to represent analysis and 30% is considered sufficient to validate the model (Silalahi et al., 2019). In this study, a total of 286 landslides were demarcated. ArcGIS 10.7 was used as mapping software to conduct a landslide susceptibility analysis that involved extracting data from high-resolution Google Earth imagery and field verification to prepare the landslide inventory map as shown in Figure 3. The dataset used in the study is shown in Table 1.

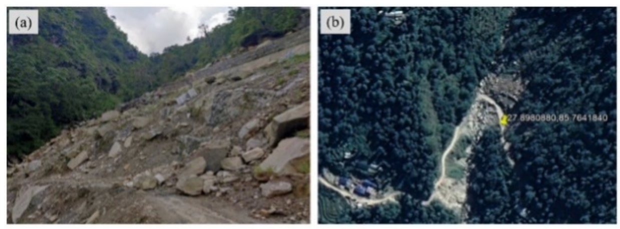

Figure 3. a) Landslide in Pantang, b)Location of landslide as seen in Google Earth

Computation of Landslide Susceptibility Index (LSI) requires calculation including the frequency ratio (FR), in which the causative factors and landslide inventory is used as presented in Equation (1).

$$FR = \frac{N_{pix(1)}/N_{pix(2)}}{\Sigma N_{pix(3)}/\Sigma N_{pix(4)}} \tag{1}$$

where, $N_{pix(1)}$ is the number of pixels containing landslide in a class, $N_{pix(2)}$ symbolises total number of pixels of each class in the whole area, $\Sigma N_{pix(3)}$ is the total number

Table 1. Dataset used for the study

Dataset	Source
Landslide Inventory	Google Earth Imagery,Site verification
DEM	Derived from ALOS Palsar, Downloaded from USGS/ Raster Grid (12.5 m x 12.5 m)
Geological Map	Geological Map of 1:1,000,000 scale published by Department of Mines and Geology
Road/Drainage	Data from Survey Department, Nepal. Scale: 1:100,000
Rainfall	Department of Hydrology & Meteorology, Nepal
Landuse	Landsat data from USGS

of pixels containing landslide and $\Sigma N_{pix(4)}$ means the total number of pixels in the study area (Yilmaz, 2009). The value greater than 1 indicates a higher correlation, while values lower than 1 indicate a lower correlation. Furthermore, the relative importance of each spatial factor with the available training dataset, called the prediction rate (PR), was determined depending upon its degree of spatial correlation with the training landslide dataset which is shown in Equation (2).

The FR model was also applied in landslide susceptibility mapping yielding a good prediction rate of 79.14%. The study also revealed that geology had the highest PR of 2.52 which played a significant role in landslide susceptibility among all the factors (Pokharel and Thapa, 2019). The Relative Frequency (RF) is a ratio of the frequency of a data point to the total size of the data set.

$$PR = \frac{RF_{max} - RF_{min}}{(RF_{max} - RF_{min})_{min}} \tag{2}$$

where, PR=Predictor Rate, RF_{max} and RF_{min} are the maximum and minimum Relative Frequency among classes within a factor respectively. Finally, the landslide susceptibility map is prepared by calculating Landslide Susceptibility Index (LSI) using the relation depicted in Equation (3).

$$LSI = \Sigma_i PR_i \times FR_i \tag{3}$$

where FR_i is the rating of each factor type and PR_i is the multiplier for each factor.

AUC (Area Under Curve) is widely used accuracy statistics to predict the models in natural hazard assessment (Begueria, 2006) and the rate obtained can explain how well the model can predict the landslide (Fabbri et al., 1999). The landslide susceptibility map prepared using training dataset was validated using the testing data by preparing AUC.

3. Causative Factors

A range of factors and their combination may influence the landslide occurrence. The selection of factors is a key step in landslide susceptibility studies. Therefore, 12 landslide causative factors are selected for this study considering field observations, data availability, and literature review.

1. **Slope**: As the slope angle increases, shear stress in the soil or other un-consolidated material generally increases (Raghuvanshi et al., 2015). The slope angle is determined from a digital elevation model (DEM) with a 12.5 m pixel. In our study, slope range of 30-40 ° and 40-50° together contribute to over 63% of demarcated landslides.
2. **Aspect**: An aspect is the direction of the slope with respect to the geographic North. Aspect associated parameters such as rainfall, drying winds, and exposure to sunlight may affect the occurrence of landslides (Pradhan and Lee, 2010). In this study, maximum landslides were observed in south facing slopes.
3. **Elevation**: Elevation affects landslides, with higher elevations having higher weathering (Varnes, 1984). In this study, 1500-2000 m elevation range had the maximum number of observed landslides.
4. **Geology**: Lithology describes the physical characteristics of a rock unit and lithological and structural changes alter the strength and permeability of rocks and soils (Dai and Lee, 2002). The geological characteristics of the study area generally are described by lithology categorized into ten units: Higher Himalayan Crystallines, Gneisses, Ulleri Formation, Lakharpata Formation, Galyang Formation, Syangja Formation, Ranimatta Formation, Ghanapokhara Formation, Kushma Formation, and Naudanda Formation. In this study, Higher Himalayan Crystallines faced maximum landslides.
5. **Land use**: Landslide occurrence as a response to landuse changes has been studied over various periods (Lambin et al., 2003). The land that is barren and sparsely vegetated is prone to weathering, erosion, and slope instability. For this study, the 'land use' has been partitioned into 6 categories: waterbodies, snow, forest, built up, barren land, and agriculture. Barren land and agriculture have faced maximum landslides in the area.
6. **Distance to Road**: Roads on slopes can disrupt support, causing strain and instability (Devkota et al., 2013).

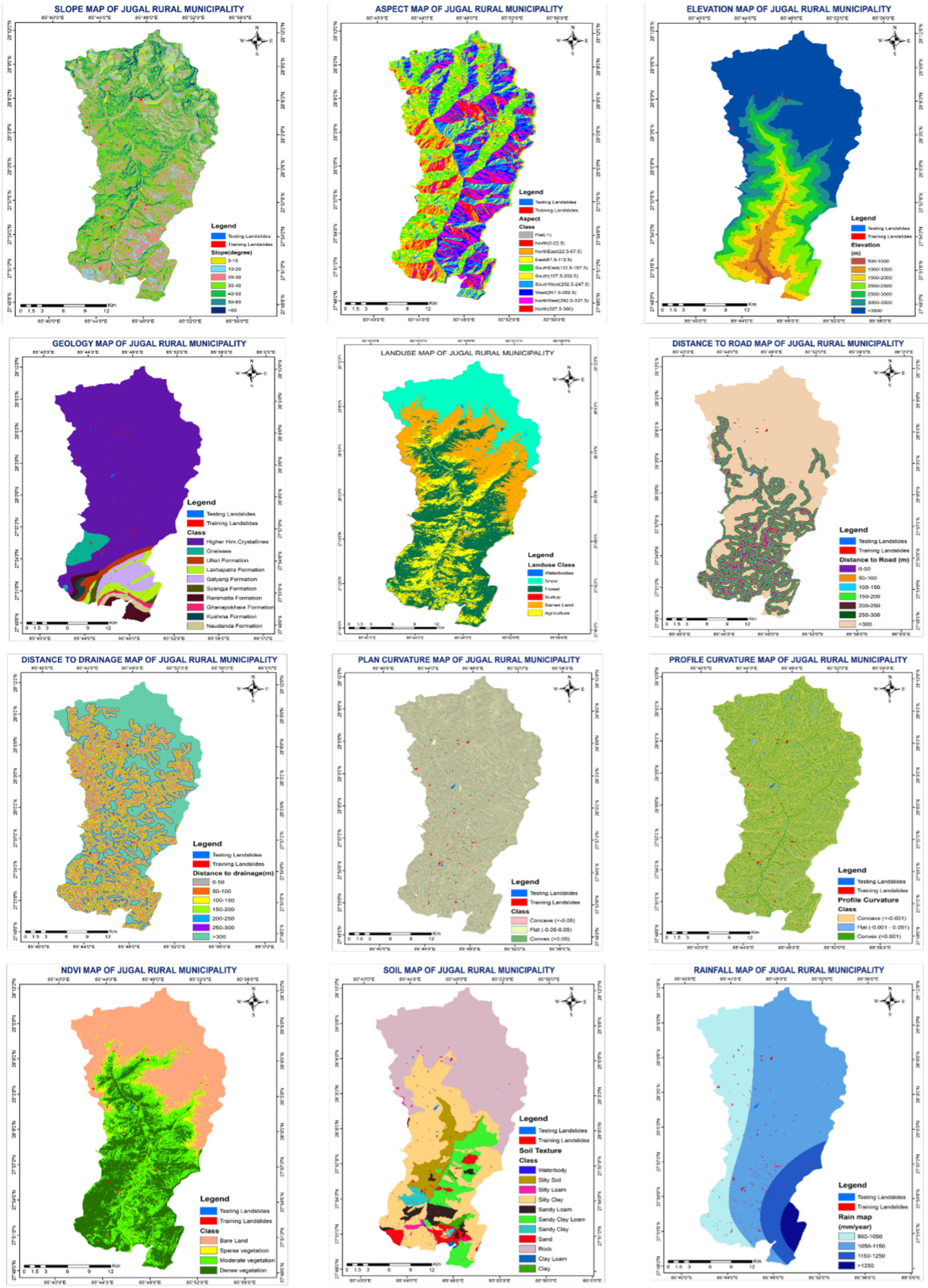

Figure 4. Different causative factor maps used for landslide susceptibility analysis

7. **Distance to Drainage**: Distance from drainage affects slope stability due to water action and erosion (Bijukchhen et al., 2013). The distance from the drainage can impact on the stability of slopes as water acts on the slopes and triggers erosion of the groundmass. In this study, 0-50 m buffer from drainage has suffered maximum landslides.
8. **Plan Curvature**: Plan curvature indicates slope shape, and profile curvature influences water flow and erosion (Ayalew and Yamagishi, 2005). In this study, concave plan curvature has shown maximum landslides.
9. **Profile Curvature**: The profile curvature is the curvature of the surface in the direction of the steepest slope i.e., in the vertical plane of a flow line (Ayalew et al., 2004). In this study, convex profile curvature has shown maximum landslides.
10. **Normalized difference Vegetation Index (NDVI)**: It assesses vegetation richness, with higher values indicating better vegetation (Gulácsi and Kovács, 2015). In this study, barren land and Moderate vegetation have shown maximum number of landslides.
11. **Soil Type**: Soil characteristics like depth, surface texture, depth texture, soil erosion, and hydraulic conductivity play significant roles in causing landslides (Sharma et al., 2012). In this study, silty clay textured soil has shown maximum landslides.
12. **Rainfall**: Rainfall increases the weight of the soil mass relative to normal conditions which reduces the amount of movement resistance resulting in slides and collapse (Dechkamfoo et al., 2022). In this study, rainfall range of 1050-1150 mm/year has encountered maximum landslides.

Different causative factor maps used for landslide susceptibility analysis in the study area in shown in Figure 4.

4. Result and Discussion

4.1. Susceptibility analysis

A higher FR indicates a stronger correlation between the conditioning factor and landslides. Slopes of 40-50 ° have the highest FR of 1.765, suggesting most landslides occur there. South-facing slopes have an FR of 1.690, indicating a higher landslide probability. Elevations between 1000-1500 m have the highest FR (2.913) for landslides. The geological unit of Gneisses is highly susceptible with an FR of 2.13. 'Built up' land use has a high FR of 2.703.

Furthermore, landslide probability is highest in areas with drainage within 0-50 m (FR 1.373). Plan and profile curvature do not significantly affect landslides as their classes' FR were found similar. Moderate vegetation (FR 1.63) dominates NDVI classes. Silty soil (FR 3.086) is the most influential among soil types, while rainfall is crucial between 1050-1150 m (FR 1.127). After FR calculations, Prediction rate (PR) of each factor is calculated which shows 'Land use' class has the highest PR: 9.35 which suggest that alterations in the land use in the study area have significant role in landslide susceptibility among all the factors. Detailed calculations and summary are shown in Figure 5 and 6.

4.2. Susceptibility map

The initial step involves reclassifying the factor maps using RF and then rating them with Probability Ratio (PR). A higher PR value indicates a more significant impact of the conditioning factor on landslide occurrences. Among these factors, 'Land use' is identified as the major factor on landslide occurrence, while 'Plan curvature' has the least impact. To create the Landslide Susceptibility Map (LSM), LSI was classified into five distinct zones using natural breaks classification in GIS: very low, low, moderate, high, and very high susceptibility zones (Figure 7). A total of 9.77% of the area lies within the very high susceptible zone, and accounts for 52.37% of the total landslides area. On the other hand, the low and very low zones cover a combined area of 50.81%, with only a 7.33% occurrence of landslides. This demonstrates the model's performance, and a detailed breakdown is provided in Figure **??**.

4.3. Validation

Area under curve (AUC) is a widely used accuracy statistics to predict the models in natural hazard assessment and the rate obtained can explain how well the model can predict the landslide (Chung and Fabbri, 2003). The landslide susceptibility map prepared using training dataset was validated using the testing data by preparing AUC. For obtaining the relative ranks, the calculated index value for each cell in study area is sorted in descending order (Dahal and Dahal, 2017). The success rate of 83.6% and prediction rate of 83.1% were obtained for the landslide susceptibility as shown in Figure 9 and Figure 10 respectively.

4.4. Discussion

A landslide susceptibility analysis was conducted by combining various factors contributing to landslides using an adjusted frequency ratio method. In this research, land use (PR= 9.35) emerged as the most influential factor in causing landslides within the study area. Several factors contributing to changes in land use were identified, including socioeconomic growth, climate change, inadequate planning, and poor plan execution. Morrow et al. (2017) have indicated that maintaining forest cover significantly reduces soil erosion rates. However, the conversion of barren land and forests into agricultural areas in hilly regions has accelerated soil erosion over time.

SN	Factors	Class	FR	RF	PR
1	**Slope**	0-10	0.401	0.059	
		10-20	0.235	0.035	
		20-30	0.625	0.092	
		30-40	1.288	0.189	
		40-50	1.765	0.260	
		50-60	1.608	0.237	
		>60	0.875	0.129	
	Total		**6.797**		**7.033**
2	**Aspect**	Flat	3.381	0.265	
		North	2.156	0.169	
		North-East	1.024	0.080	
		East	0.849	0.066	
		South-East	1.153	0.090	
		South	1.690	0.132	
		South-West	1.259	0.099	
		West	0.317	0.025	
		Northwest	0.240	0.019	
		North	0.707	0.055	
	Total		**12.776**		**7.678**
3	**Elevation (m)**	500-1000	0.546	0.056	
		1000-1500	2.913	0.297	
		1500-2000	2.792	0.284	
		2000-2500	0.713	0.073	
		2500-3000	1.014	0.103	
		3000-3500	1.515	0.154	
		>3500	0.330	0.034	
	Total		**9.822**		**8.214**
4	**Geology**	Higher Him. Cryst.	0.912	0.080	
		Gneisses	2.130	0.187	
		Ulleri Formation	1.898	0.167	
		Lakharpata Formation	2.102	0.185	
		Galyang Formation	0.560	0.049	
		Syangja Formation	0.238	0.021	
		Ranimatta Formation	1.384	0.122	
		Ghanapok-hara Form.	1.811	0.159	
		Kushma Formation	0.092	0.008	
		Naudanda Formation	0.260	0.023	
	Total		**11.386**		**5.188**
5	**Land use pattern**	Waterbodies	1.316	0.157	
		Barren Land	1.482	0.177	
		Forest	0.482	0.057	
		Agriculture	2.221	0.265	
		Snow	0.190	0.023	
		Builtup	2.703	0.322	
	Total		**20.694**		**9.350**

SN	Factors	Class	FR	RF	PR
6	**Distance to Road (m)**	0-50	1.336	0.156	
		50-100	1.336	0.156	
		100-150	1.278	0.150	
		150-200	1.214	0.142	
		200-250	1.121	0.131	
		250-300	1.420	0.166	
		>300	0.839	0.098	
	Total		**8.544**		**2.122**
7	**Distance to Drainage (m)**	0-50	1.373	0.174	
		50-100	1.229	0.156	
		100-150	1.303	0.166	
		150-200	1.242	0.158	
		200-250	1.165	0.148	
		250-300	1.173	0.149	
		>300	0.390	0.050	
	Total		**7.875**		**3.898**
8	**Plan Curvature**	Concave	1.050	0.354	
		Flat	0.955	0.322	
		Convex	0.960	0.324	
	Total		**2.966**		**1.000**
9	**Profile Curvature**	Concave	0.971	0.335	
		Flat	0.892	0.307	
		Convex	1.039	0.358	
	Total		**2.901**		**1.582**
10	**NDVI**	Bare Land	0.900	0.197	
		Sparse veg.	1.552	0.339	
		Moderate veg.	1.632	0.357	
		Dense veg.	0.489	0.107	
	Total		**4.574**		**7.809**
11	**Soil Type**	Sandy Loam	1.308	0.090	
		Sandy Clay Loam	1.516	0.105	
		Silty Clay	1.166	0.080	
		Sand	1.703	0.117	
		Sandy Clay	2.467	0.170	
		Silty Soil	3.086	0.213	
		Silty Loam	1.572	0.108	
		Clay Loam	0.000	0.000	
		Clay	0.247	0.017	
		Rock	0.393	0.027	
		Waterbody	1.046	0.072	
	Total		**14.504**		**6.644**
12	**Rainfall (mm/yr)**	950-1050	0.925	0.307	
		1050-1150	1.127	0.375	
		1150-1250	0.633	0.210	
		>1250	0.323	0.107	
	Total		**3.009**		**8.346**

Figure 5. Calculation tables for FR, RF, and PR

Additionally, a separate study in Wanzhou County, China, investigated the individual and combined effects of land use changes on slope stability and found that climate change had a more detrimental impact on landslide susceptibility compared to the stabilizing effect of land use changes. Consequently, the future stability of the study area

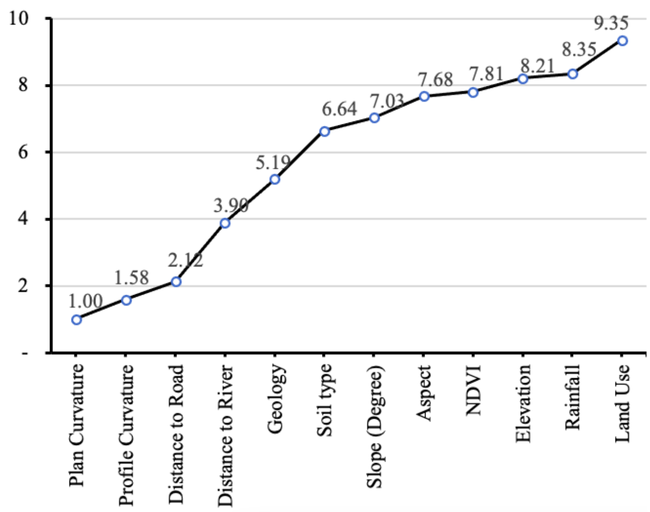

Figure 6. Landslide affecting factors with their corresponding Predication Rate (PR)

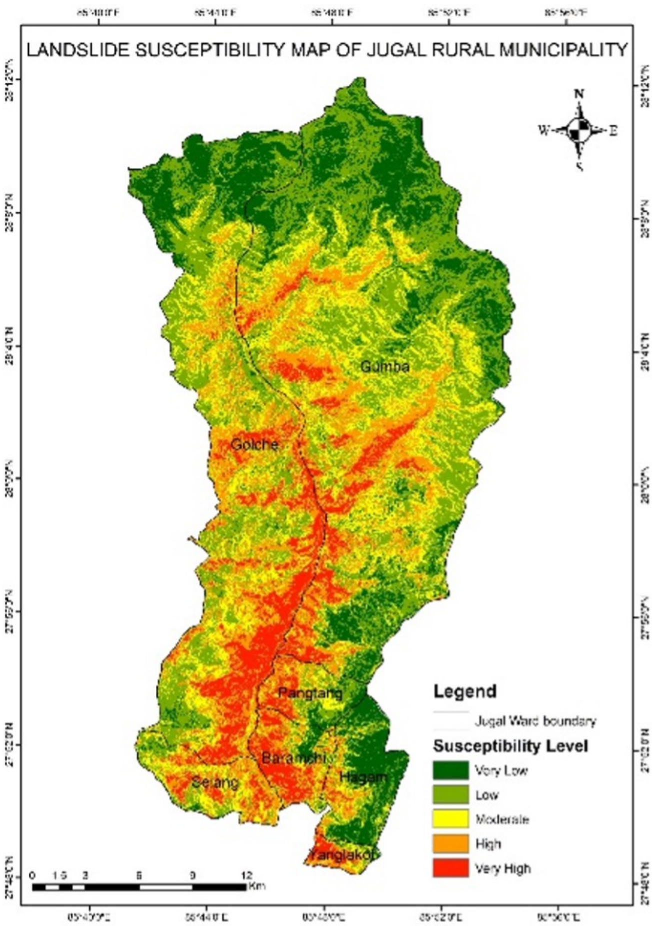

Figure 7. LSM of Jugal Rural Municipality

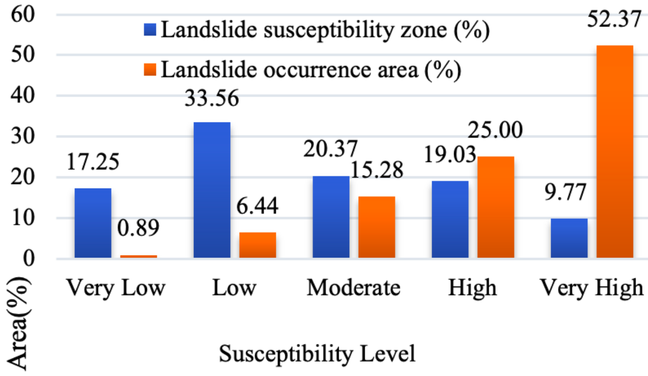

Figure 8. Comparison of Landslide susceptibility zone (%) and Landslide occurrence area (%)

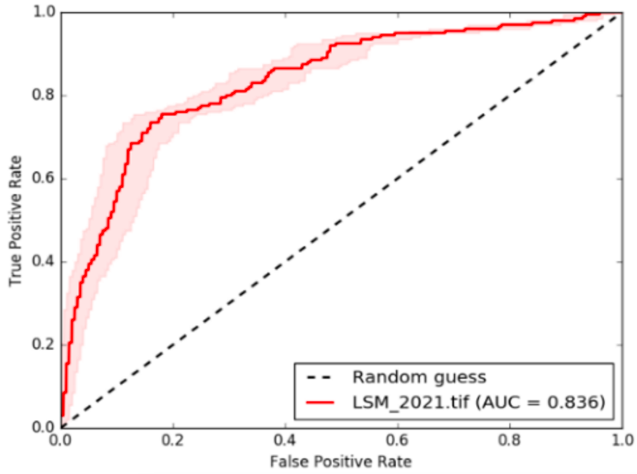

Figure 9. AUC for success rate calculated using training data

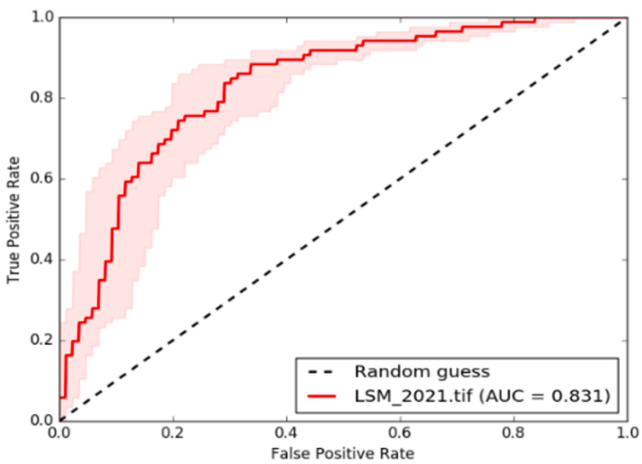

Figure 10. AUC for prediction rate calculated using testing data

is expected to decrease (Guo et al., 2023).

Our study shows that among the land use classes, 'agriculture', 'built up', and 'barren land' have high FR and as a result, alterations in these factors will directly impact the landslide susceptibility. As the needs of the population evolve over time, there is a growing demand for essential amenities such as food, housing, healthcare, education, electricity, water supply, roads, and irrigation. To meet this demand, numerous infrastructures have been constructed, resulting in an increase in built-up areas and a reduction in forested land. The decrease in forested land can also be attributed to encroachment, which occurs due to weak enforcement and implementation of laws and policies.

5. Conclusion

Landslide susceptibility assessment of Jugal Rural Municipality, Sindhupalchok has been carried out using Modified Frequency Ratio (FR) model considering landslide inventory and conditioning factors of landslides for preparing LSM. Twelve conditioning factors were collected and prepared into a spatial database using GIS for evaluation of the spatial relationship between these factors and landslide occurrences using modified Frequency Ratio (FR) model. The success and prediction rate of 83.60% and 83.10%, respectively, infer that FR model fits well for the study area. The prediction rate indicated that 'Land use' factor is the most significant factor in affecting the landslide susceptibility of the study area. Critical facilities such as schools, shelters, hospitals, bridges, and roads that lie in higher landslide susceptible zone should be prioritized, properly examined with detail engineering and geotechnical consideration using experts to mitigate future losses. The prepared landslide susceptibility map of the region can be helpful for understanding consequences of future land use changes and support decision makers for land use planning and landslide risk mitigation.

References

Ayalew, L., H., Y., & Ugawa, N. (2004). Landslide susceptibility mapping using GIS-based weighted linear combination, the case in Tsugawa area of Agano river, Niigata prefecture, Japan. *Landslides*, *1*(1), 73–81. https://doi.org/10.1007/s10346-003-0006-9

Ayalew, L., & Yamagishi, H. (2005). The application of gis-based logistic regression for landslide susceptibility mapping in the Kakuda-Yahiko mountains, central Japan. *Geomorphology*, *65*(1-2), 15–31. https://doi.org/10.1016/j.geomorph.2004.06.010

Begueria, S. (2006). Validation and evaluation of predictive models in hazard assessment and risk management. *Natural Hazards*, *37*(3). https://doi.org/10.1007/s11069-005-5182-6

Bhusal, R. (2016). Hazards in the high mountains: Koshi basin part i. *The Wire*.

Bijukchhen, S., Kayastha, P., & Dhital, M. (2013). A comparative evaluation of heuristic and bivariate statistical modelling for landslide susceptibility mappings in Ghurmi–Dhad khola, east Nepal. *Arabian Journal of Geosciences*, *6*(8), 2727–2743. https://doi.org/10.1007/s12517-012-0569-7

Chung, C., & Fabbri, A. (2003). Validation of spatial prediction models for landslide hazard mapping. *Problemy Peredachi Informatsii*, *40*(2).

Dahal, B., & Dahal, R. (2017). Landslide hazard map: Tool for optimization of low-cost mitigation. *Geoenvironmental Disasters*, *4*(1), 8. https://doi.org/10.1186/s40677-017-0071-3

Dai, F., & Lee, F. (2002). Landslide characteristics and slope instability modeling using GIS, Lantau island, HongKong. *Geomorphology*, *42*, 213–228.

Dechkamfoo, C., Sitthikankun, S., T., K. N. A., Manokeaw, S., Timprae, W., Tepweerakun, S., Tengtrairat, N., Aryupong, C., Jitsangiam, P., & Rinchumphu, D. (2022). Impact of rainfall-induced landslide susceptibility risk on mountain roadside in northern Thailand. *Infrastructures*, *7*, 17. https://doi.org/10.3390/infrastructures7020017

Devkota, K. C., Regmi, A. D., Pourghasemi, H. R., Yoshida, K., Pradhan, B., Ryu, I. C., Dhital, M. R., & Althuwaynee, O. F. (2013). Landslide susceptibility mapping using certainty factor, index of entropy and logistic regression models in GIS and their comparison at Mugling–Narayanghat road section in Nepal Himalaya. *Natural Hazards*, *65*(1), 135–165. https://doi.org/10.1007/s11069-012-0347-6

Fabbri, A., Chung, C.-J. F., & Fabbri, A. G. (1999). Probabilistic prediction models for landslide hazard mapping. *Photogrammetric Engineering Remote Sensing'*, *65*(12), 1389–1399.

Gulácsi, A., & Kovács, F. (2015). Reconfiguration of distribution network for loss reduction and reliability improvement based on an enhanced genetic algorithm. *International Journal of Electrical Power & Energy Systems*, *8*(3-4), 11–20. https://doi.org/10.1515/jengeo-2015-0008

Guo, Z., Ferrer, J. V., Hürlimann, M., Medina, V., Puig-Polo, C., Yin, K., & Huang, D. (2023). Shallow landslide susceptibility assessment under future climate and land cover changes: A case study from southwest China. *Geoscience Frontiers*, *14*(4), 101542. https://doi.org/10.1016/j.gsf.2023.101542

Lambin, E. F., Geist, H. J., & Lepers, E. (2003). Dynamics of land-use and land-cover change in tropical regions. *Annual Review of Environment and Resources*, *28*, 205–241. https://doi.org/10.1146/annurev.energy.28.050302.105459

Martha, T. R., van Westen, C. J., Kerle, N., Jetten, V., & Vinod Kumar, K. (2013). Landslide hazard and risk assessment using semi-automatically created landslide inventories. *Geomorphology*, *184*, 139–150. https://doi.org/10.1016/j.geomorph.2012.12.001

McAdoo, B. G., Quak, M., Gnyawali, K. R., Adhikari, B. R., Devkota, S., Lal Rajbhandari, P., & Sudmeier-Rieux, K. (2018). Roads and landslides in Nepal: How development affects environmental risk. *Natural Hazards and Earth System Sciences*, *18*(12), 3203–3210. https://doi.org/10.5194/nhess-18-3203-2018

MoHA. (2020). *Landslide incident record* (tech. rep.). Disaster Risk Reduction Portal.

MoHA. (2022). *Risk profile of Nepal* (tech. rep.). Disaster Risk Reduction Portal.

Morrow, S., Smolen, J., M.and Stiegler, & Cole, J. (2017). *Using vegetation for erosion control on construction sites* (tech. rep.). Oakstate.edu.

Paudyal, P., Dahal, P., Bhandari, P., & Dahal, B. K. (2023). Sustainable rural infrastructure: Guidelines for roadside slope excavation. *Geoenvironmental Disasters*, *10*(1), 11. https://doi.org/10.1186/s40677-023-00240-x

Pokharel, B., & Thapa, P. B. (2019). Landslide susceptibility in Rasuwa district of central Nepal after the 2015 Gorkha earthquake. *Journal of Nepal Geological Society*, *59*, 79–88. https://doi.org/10.3126/jngs.v59i0.24992

Pradhan, B., & Lee, S. (2010). Delineation of landslide hazard areas on Penang island, Malaysia, by using frequency ratio, logistic regression, and artificial neural network models. *Environmental Earth Sciences*, *60*(5), 1037–1054. https://doi.org/10.1007/s12665-009-0245-8

Raghuvanshi, T. K., Negassa, L., & Kala, P. M. (2015). GIS based grid overlay method versus modeling approach - a comparative study for landslide hazard zonation (LHZ) in Meta Robi district of west Showa zone in Ethiopia. *Electric Power Systems Research*, *18*(2), 235–250. https://doi.org/10.1016/j.ejrs.2015.08.001

Regmi, A. D., Devkota, K. C., Yoshida, K., Pradhan, B., Pourghasemi, H. R., Kumamoto, T., & Akgun, A. (2014). Application of frequency ratio, statistical index, and weights-of-evidence models and their comparison in landslide susceptibility mapping in central Nepal Himalaya. *Arabian Journal of Geosciences*, *7*(2), 725–742. https://doi.org/10.1007/s12517-012-0807-z

Sharma, L. P., Patel, N., Debnath, P., & Ghose, M. K. (2012). Assessing landslide vulnerability from soil characteristics-a GIS-based analysis. *Arabian Journal of Geosciences*, *5*(4), 789–796. https://doi.org/10.1007/s12517-010-0272-5

Silalahi, F. E. S., Pamela, A. Y., & Hidayat, F. (2019). Landslide susceptibility assessment using frequency ratio model in Bogor, west Java, Indonesia. *Geosciences Letters*, *6*(1). https://doi.org/10.1186/s40562-019-0140-4

Sönke, K., Eckstein, D., Dorsch, L., & Fischer, L. (2015). *Global climate risk index 2016: Who suffers most from extreme weather events? weather-related loss events in 2014 and 1995 to 2014* (tech. rep.). Germanwatch.

Thapa, S., Karna, A. K., & Dahal, B. K. (2022). Evaluation of different landslide susceptibility analysis methods: A case study of Bagmati rural municipality. *Journal of Engineering Technology and Planning*, *3*(1), 44–59. https://doi.org/10.3126/joetp.v3i1.49607

Uprety, D. R., Shrestha, K., & Svensson, A. (2020). *Nepal's deadly landslides explained* (tech. rep.). Preventionweb.

Varnes, D. J. (1984). *Landslide hazard zonation: A review of principles and practice* (tech. rep.). UNESCO.

Yilmaz, I. (2009). Landslide susceptibility mapping using frequency ratio, logistic regression, artificial neural networks and their comparison: A case study from Kat landslides (Tokat—Turkey). *Computers Geosciences*, *35*(6), 1125–1138.

This work is licensed under a Creative Commons "Attribution-NonCommercial-NoDerivatives 4.0 International" license.